

# Positronium scattering by atomic hydrogen with inclusion of target excitation channels

Jennifer E. Blackwood,<sup>1</sup> Mary T. McAlinden,<sup>2</sup> and H. R. J. Walters<sup>1</sup>

<sup>1</sup>*Department of Applied Mathematics and Theoretical Physics, Queen's University, Belfast BT7 1NN, United Kingdom*

<sup>2</sup>*School of Computing and Mathematical Sciences, Oxford Brookes University, Wheatley Campus, Oxford OX33 1HX, United Kingdom*

(Received 21 September 2001; published 27 February 2002)

Calculations are reported for positronium (Ps) scattering by atomic hydrogen (H) in the energy range 0–6.5 eV in a coupled-pseudostate approximation in which excitation and ionization channels of both the Ps and the H are taken into account. The approximation contains an accurate representation of the van der Waals coefficient. Results are presented for phase shifts, scattering lengths, effective ranges, and various cross sections including partial wave, total, and ortho-para conversion cross sections. An analysis of the possible spin transitions is provided and the energy of the positronium hydride (PsH) bound state is determined. Substantial differences are found from earlier work within the frozen target approximation, now clearly confirming the importance of target excitation channels. Good agreement is obtained with recent calculations of *S*-wave phase shifts and scattering lengths using the stabilization method. Convergence to the exact binding energy for PsH appears to be slow. Resonances corresponding to unstable states of the positron orbiting  $H^-$  are seen in the electronic spin singlet partial waves. The importance of the  $H^-$  formation channel is discussed.

DOI: 10.1103/PhysRevA.65.032517

PACS number(s): 36.10.Dr, 34.50.-s

## I. INTRODUCTION

The development of energy tunable positronium (Ps) beams [1–15] has fuelled interest in Ps scattering by atoms and molecules [16]. Measurements of total cross sections have been made for He, Ar,  $H_2$ , and  $O_2$  targets [10,13,14] and also some rough data have been obtained on differential scattering by He, Ar, and  $H_2$  [13,14]. Positronium comes in two spin states, singlet [called para (*p*)-Ps] and triplet [called ortho (*o*)-Ps]. These states have radically different lifetimes, thus *o*-Ps( $1s$ ) has a lifetime of 142 ns while *p*-Ps( $1s$ ) has a lifetime of 0.125 ns. This lifetime results from electron-positron annihilation into photons, predominantly two photons in the case of *p*-Ps( $1s$ ) and three in the case of *o*-Ps( $1s$ ). As our notation suggests, it is necessary also to define the electronic state of the Ps, e.g.,  $1s$ ,  $2s$ ,  $2p$ , etc. Present day beams consist essentially of *o*-Ps in the ground state, i.e., *o*-Ps( $1s$ ). In addition to the beam measurements, some low-energy cross-section data have been deduced by modeling the annihilation of *o*-Ps( $1s$ ) in various gases [4,17–21].

The simplest Ps-atom system, and a prototype for all other cases, is Ps-H. Besides relative simplicity, it has the advantage that the wave functions of the target, i.e., H, are known exactly and so results cannot be clouded by issues of inexact target representation. It has the disadvantage of not being experimentally amenable now, nor seemingly in the immediate future. The earliest theoretical foray into Ps-H scattering [22] goes back to Massey and Mohr [23] who tried to make some progress using the first Born approximation (FBA). A more recent first Born study is reported in [24]. While Massey and Mohr realized the importance of electron exchange in low-energy Ps-H elastic scattering, they also appreciated that this interaction was too strong to be handled within the context of the FBA. A nonperturbative treatment of electron exchange was made by Fraser [25] who employed the static-exchange approximation. More recent applications of the static-exchange approximation to Ps-H scattering may be

found in [26,27]. Static-exchange is but the simplest form of a coupled-state approximation, see Eq. (2), in which only the single term involving the initial states of the Ps and the atom is retained.

*S*-wave scattering, which is dominant in the limit of zero impact energy, has received much attention. Thus, Drachman and Houston [28,29] have used the stabilization method [30] to calculate scattering lengths and effective ranges as well as phase shifts at a few isolated energies. This approach has very recently been updated by Ivanov, Mitroy, and Varga [31]. Scattering lengths have also been calculated by Page [32] using the Kohn variational principle and, again very recently, by Adhikari and Mandal [33] using a different variational functional. In the latter case, however, the variational result has been compromised by neglect of an off-shell contribution from a Green's function.

The *S*-wave symmetry is also of considerable interest because, in its electronic spin singlet state, it possesses a bound state, positronium hydride (PsH), and resonance structure. The existence of PsH was first demonstrated theoretically by Ore [34], the most up-to-date value for its binding energy is 1.067 eV [35]. Resonance structure in the *S* wave was described by Drachman and Houston [28]. Drachman [36] went on to interpret this structure as corresponding to unstable states of the positron orbiting the  $H^-$  ion. This interpretation explains why resonances are seen only in the electronic spin singlet channel ( $H^-$  only exists in the singlet state), it also implies that resonances should appear in *P*, *D*, and higher waves, which indeed they do [27,35,37–39]. Using the complex coordinate rotation method, Yan and Ho have identified three *S*-wave resonances [35], two *P*-wave resonances [37] and one resonance in each of the *D*, *F*, and *G* waves [38,39]. These are but the lowest members of an infinite series of Rydberg resonances in each partial wave converging on to the  $H^-$  formation threshold at 6.05 eV as the model of Drachman [36] requires. These series have now been made explicitly visible in recent scattering calculations by Blackwood, McAlinden, and Walters [40]. According to Ho [41]

there should also be series converging to thresholds for excited (unstable)  $H^-$  formation, e.g.,  $H^-(2s^2)$ , while, according to Blackwood, McAlinden, and Walters [40], there should be series converging to the  $Ps^-$  formation threshold at 13.3 eV corresponding to unstable Rydberg orbits of  $Ps^-$  (an electronic spin singlet) about the proton.

In recent years the main thrust of theoretical work on Ps-atom scattering has been in the direction of coupled-state methods [16,24,27,42–70]. Here the collisional wavefunction  $\Psi$ , is expanded in a product of Ps and atom states [see Eq. (2)]. Such methods scale (badly) as the product of the number of Ps states times the number of atom states. Since Ps (ionization potential 6.8 eV) is usually a more fragile object than the atom target [e.g.,  $H(1s)$ , ionization potential 13.6 eV] it has seemed reasonable, at least in the first instance, to adopt a frozen target approximation, i.e., to retain in the expansion for  $\psi$  only those terms involving the initial atomic state  $\psi_0$ . To complete the picture, the FBA (or Born-Oppenheimer approximation) would then be used to take account of collisions in which the atom is excited or ionized [24,27,53,66]. The largest calculation of Ps-H scattering within the frozen target framework is the 22 (Ps) state approximation reported by Campbell *et al.* [27] which includes pseudostates to represent ionization channels of the Ps. This approximation produces a PsH state with a binding energy of 0.634 eV, i.e., 60% of the exact value [35], and exhibits resonance structure in the electronic spin singlet  $S$ ,  $P$ ,  $D$ , and higher partial waves, but at energies typically 0.57 eV higher than the accurate results of Yan and Ho [35,37–39]. At least at low-impact energies, there is evidence that this 22 state approximation is close to a converged answer within the context of the frozen target approximation. If this is indeed so, then the substantive discrepancies in the PsH binding energy and the resonance positions clearly point to the importance of the neglected H states, i.e., to target excitation [71], in the expansion for  $\Psi$ .

It is the purpose of this paper to investigate the significance of this omission in  $Ps(1s) + H(1s)$  scattering in the low-energy region from 0 to 6.5 eV. In this region real excitation of the atom is not possible, but virtual excitation of the target through the coupled equations can make itself felt [16]. Virtual target excitation brings in additional physics, in particular it introduces [72] the van der Waals interaction

$$-\frac{C_6}{R^6}, \quad (1)$$

which is the leading long-range interaction between  $Ps(1s)$  and  $H(1s)$  at separation  $R$ . This interaction requires simultaneous excitation of the  $Ps(1s)$  and the  $H(1s)$  to intermediate  $p$  states and is therefore not representable within the frozen target approximation. In atomic units  $C_6$  has the value 34.784 73 [73] and so is relatively large.

This is not the first investigation into target excitation effects. Earlier work, most notably by the Calcutta group of Ghosh *et al.*, may be found in [44,46,47,49,51,56,57,64–67,70], but is on a much smaller scale than that presented here. Noteworthy are two recent publications by Ghosh and collaborators on target excitation in  $o$ - $Ps(1s)$ -He scattering

[65,66], these show a substantial drop in the low-energy elastic cross section (by a factor of two) on the mere addition of the two eigenstates  $He(2^1S)$  and  $He(2^1P)$ . Here, however, one must ask questions about sensitivity to the use of approximate wave functions, an issue that was of importance even in the simpler problem of positron-He scattering [74,75]. That issue does not arise in the  $Ps(1s)$ - $H(1s)$  system studied here.

Throughout this paper we shall use atomic units (a.u.) in which  $\hbar = m_e = e = 1$ . The symbol  $a_0$  will denote the Bohr radius.

## II. THEORY

The coupled-state expansion for Ps-H scattering takes the form

$$\begin{aligned} \Psi^{(S_e)} = \sum_{a,b} [G_{ab}^{(S_e)}(\mathbf{R}_1) \phi_a(\mathbf{t}_1) \psi_b(\mathbf{r}_2) \\ + (-1)^{S_e} G_{ab}^{(S_e)}(\mathbf{R}_2) \phi_a(\mathbf{t}_2) \psi_b(\mathbf{r}_1)], \quad (2) \end{aligned}$$

where the sum is over Ps states  $\phi_a$  and H states  $\psi_b$ ,  $\mathbf{r}_p$  ( $\mathbf{r}_i$ ) is the position vector of the positron ( $i$ th electron) relative to the proton,  $\mathbf{R}_i \equiv (\mathbf{r}_p + \mathbf{r}_i)/2$  is the Ps (i.e., positron plus  $i$ th electron) center-of-mass coordinate,  $\mathbf{t}_i \equiv \mathbf{r}_p - \mathbf{r}_i$  is the Ps internal coordinate, and  $S_e (= 0, 1)$  is the total electronic spin, which is conserved in the collision. The positron spin is separately conserved. The states  $\phi_a$  and  $\psi_b$  may be either eigenstates or pseudostates, it is assumed that they satisfy

$$\begin{aligned} \langle \phi_a(\mathbf{t}) | H_{Ps}(\mathbf{t}) | \phi_{a'}(\mathbf{t}) \rangle &= E_a \delta_{aa'}, \\ \langle \phi_a(\mathbf{t}) | \phi_{a'}(\mathbf{t}) \rangle &= \delta_{aa'}, \quad (3) \end{aligned}$$

$$\begin{aligned} \langle \psi_b(\mathbf{r}) | H_H(\mathbf{r}) | \psi_{b'}(\mathbf{r}) \rangle &= \varepsilon_b \delta_{bb'}, \\ \langle \psi_b(\mathbf{r}) | \psi_{b'}(\mathbf{r}) \rangle &= \delta_{bb'}, \quad (4) \end{aligned}$$

where

$$H_{Ps}(\mathbf{t}) \equiv -\nabla_t^2 - \frac{1}{t} \quad (5)$$

is the Ps Hamiltonian, and

$$H_H(\mathbf{r}) \equiv -\frac{1}{2} \nabla_r^2 - \frac{1}{r} \quad (6)$$

is the Hamiltonian for the H atom.

The full Hamiltonian for the Ps-H system is

$$\begin{aligned} H &= -\frac{1}{4} \nabla_{R_1}^2 + H_{Ps}(\mathbf{t}_1) + H_H(\mathbf{r}_2) + V_{Ps}(\mathbf{R}_1, \mathbf{t}_1; \mathbf{r}_2) \\ &= -\frac{1}{4} \nabla_{R_2}^2 + H_{Ps}(\mathbf{t}_2) + H_H(\mathbf{r}_1) + V_{Ps}(\mathbf{R}_2, \mathbf{t}_2; \mathbf{r}_1), \quad (7) \end{aligned}$$

where

$$V_{\text{Ps}}(\mathbf{R}, \mathbf{t}; \mathbf{r}) \equiv \left( \frac{1}{\left| \mathbf{R} + \frac{1}{2} \mathbf{t} \right|} - \frac{1}{\left| \mathbf{R} + \frac{1}{2} \mathbf{t} - \mathbf{r} \right|} \right) - \left( \frac{1}{\left| \mathbf{R} - \frac{1}{2} \mathbf{t} \right|} - \frac{1}{\left| \mathbf{R} - \frac{1}{2} \mathbf{t} - \mathbf{r} \right|} \right) \quad (8)$$

is the interaction between the Ps and the H atom. Coupled equations for the coefficients  $G_{ab}^{(S_e)}$  in Eq. (2) are obtained by substituting Eq (2) into the Schrödinger equation, with the Hamiltonian (7), and projecting with  $\phi_a(\mathbf{t}_1)\psi_b(\mathbf{r}_2)$ , we obtain

$$\begin{aligned} & (\nabla_{\mathbf{R}_1}^2 + p_{ab}^2) G_{ab}^{(S_e)}(\mathbf{R}_1) \\ &= 4 \sum_{a'b'} U_{ab,a'b'}(\mathbf{R}_1) G_{a'b'}^{(S_e)}(\mathbf{R}_1) + 4(-1)^{S_e} \\ & \times \sum_{a'b'} \int L_{ab,a'b'}(\mathbf{R}_1, \mathbf{R}_2) G_{a'b'}^{(S_e)}(\mathbf{R}_2) d\mathbf{R}_2, \end{aligned} \quad (9)$$

where

$$\frac{p_{ab}^2}{4} + E_a + \varepsilon_b = E, \quad (10)$$

$E$  being the total energy,

$$\begin{aligned} & U_{ab,a'b'}(\mathbf{R}_1) \\ & \equiv \langle \phi_a(\mathbf{t}_1)\psi_b(\mathbf{r}_2) | V_{\text{Ps}}(\mathbf{R}_1, \mathbf{t}_1; \mathbf{r}_2) | \phi_{a'}(\mathbf{t}_1)\psi_{b'}(\mathbf{r}_2) \rangle \end{aligned} \quad (11)$$

and

$$\begin{aligned} & \int L_{ab,a'b'}(\mathbf{R}_1, \mathbf{R}_2) G_{a'b'}^{(S_e)}(\mathbf{R}_2) d\mathbf{R}_2 \\ &= \int_{\text{fixed } \mathbf{R}_1} \phi_a^*(\mathbf{t}_1)\psi_b^*(\mathbf{r}_2) \\ & \times (H - E) G_{a'b'}^{(S_e)}(\mathbf{R}_2) \phi_{a'}(\mathbf{t}_2)\psi_{b'}(\mathbf{r}_1) d\mathbf{t}_1 d\mathbf{r}_2, \end{aligned} \quad (12)$$

where the asterisk stands for complex conjugation. The potential (11) gives the direct Coulombic interaction between the Ps and the H atom. From Eqs. (8) and (11) it is a simple matter to see that this potential is zero if the Ps states  $\phi_a$  and  $\phi_{a'}$  have the same parity. This has the consequence of weakening the direct interaction (11) relative to the electron exchange interaction (12) between the Ps and the H atom, this interaction has no zero symmetries.

The coupled Eqs. (9) are solved subject to the boundary conditions [76]

$$G_{ab}^{(S_e)}(\mathbf{R}_1) \xrightarrow{R_1 \rightarrow \infty} e^{i\mathbf{p}_0 \cdot \mathbf{R}_1} \delta_{a,0} \delta_{b,0} + f_{ab}^{(S_e)}(\hat{\mathbf{R}}_1) \frac{e^{ip_{ab}R_1}}{R_1}, \quad (13)$$

TABLE I. Cross sections for different spin combinations of Ps and H.

Initial state <sup>a,b</sup>			Final state <sup>a,b</sup>			Cross section <sup>c</sup>
Ps state	$m_{\text{Ps}}$	$m_{\text{H}}$	Ps state	$m_{\text{Ps}}$	$m_{\text{H}}$	
$p$	0	$\pm 1/2$	$p$	0	$\pm 1/2$	$A$
			$o$	$\pm 1$	$\mp 1/2$	$2B$
			$o$	0	$\pm 1/2$	$B$
$o$	$\pm 1$	$\pm 1/2$	$o$	$\pm 1$	$\pm 1/2$	$C$
$o$	$\pm 1$	$\mp 1/2$	$p$	0	$\pm 1/2$	$2B$
			$o$	$\pm 1$	$\mp 1/2$	$D$
			$o$	0	$\pm 1/2$	$2B$
$o$	0	$\pm 1/2$	$p$	0	$\pm 1/2$	$B$
			$o$	$\pm 1$	$\mp 1/2$	$2B$
			$o$	0	$\pm 1/2$	$A$

<sup>a</sup> $o(p) \equiv$  ortho (para).

<sup>b</sup> $m_{\text{Ps}}(m_{\text{H}}) \equiv$  spin component of Ps (H).

<sup>c</sup> $A, B, C,$  and  $D$  are defined in Eqs. (16)–(19).

where we assume that the Ps in the state  $\phi_0$  is incident upon the atom in the state  $\psi_0$  with momentum  $\mathbf{p}_0$ . Then,  $f_{ab}^{(S_e)}$  is the scattering amplitude in the electronic spin state  $S_e$ . If the initial spin state of the Ps (atom) is  $\chi_0(\zeta_0)$  and its final spin state is  $\chi(\zeta)$ , then it is not difficult to show that the appropriate scattering amplitude for a transition  $\phi_0\psi_0 \rightarrow \phi_a\psi_b$  is

$$\begin{aligned} g_{ab} = \frac{1}{2} \{ & \langle \chi(p,1)\zeta(2) | \chi_0(p,1)\zeta_0(2) \rangle (f_{ab}^{(0)} + f_{ab}^{(1)}) \\ & - \langle \chi(p,1)\zeta(2) | \chi_0(p,2)\zeta_0(1) \rangle (f_{ab}^{(0)} - f_{ab}^{(1)}) \}, \end{aligned} \quad (14)$$

where it is assumed that all spin functions are normalized and where  $p, 1,$  and  $2$  stand for the spin coordinates of the positron and the two electrons, respectively. The corresponding differential cross section is

$$\frac{d\sigma_{ab}}{d\Omega} = \frac{p_{ab}}{p_0} |g_{ab}|^2. \quad (15)$$

Table I shows the cross section (15) for all possible spin combinations in the initial and final states. In this table

$$A \equiv \frac{1}{16} \frac{p_{ab}}{p_0} |f_{ab}^{(0)} + 3f_{ab}^{(1)}|^2, \quad (16)$$

$$B \equiv \frac{1}{16} \frac{p_{ab}}{p_0} |f_{ab}^{(0)} - f_{ab}^{(1)}|^2, \quad (17)$$

$$C \equiv \frac{p_{ab}}{p_0} |f_{ab}^{(1)}|^2, \quad (18)$$

$$D \equiv \frac{1}{4} \frac{p_{ab}}{p_0} |f_{ab}^{(0)} + f_{ab}^{(1)}|^2. \quad (19)$$

Present day  $o$ -Ps beams are spin polarized. The origin of this polarization lies with the positron source, usually  $\text{Na}^{22}$

[13], which emits highly polarized positrons. To form a Ps beam, these positrons are first moderated to much lower energies and then passed through some suitable gas, e.g., H<sub>2</sub> [13], to pick up electrons and form Ps. By virtue of the fact that the positrons are polarized, the resultant *o*-Ps beam is also polarized. However, if this beam is directed at an unpolarized H target and if the spin orientations of the Ps and H in the final state are not measured, then from Table I it is easy to show that the appropriate cross sections are [77]

$$\frac{d\sigma_{ab}}{d\Omega}(o \rightarrow p) = \frac{1}{16} \frac{p_{ab}}{p_0} |f_{ab}^{(0)} - f_{ab}^{(1)}|^2, \quad (20)$$

$$\frac{d\sigma_{ab}}{d\Omega}(o \rightarrow o + p) = \frac{1}{4} \frac{p_{ab}}{p_0} (|f_{ab}^{(0)}|^2 + 3|f_{ab}^{(1)}|^2), \quad (21)$$

$$\frac{d\sigma_{ab}}{d\Omega}(o \rightarrow o) = \frac{d\sigma_{ab}}{d\Omega}(o \rightarrow o + p) - \frac{d\sigma_{ab}}{d\Omega}(o \rightarrow p), \quad (22)$$

where the notation  $o \rightarrow p$ , etc., distinguishes whether the final state of the Ps is ortho or para. An important point to note is that results (20) to (22) are independent of the state of polarization of the *o*-Ps beam. For the sake of completeness, we also note the corresponding cross sections for a *p*-Ps projectile

$$\frac{d\sigma_{ab}}{d\Omega}(p \rightarrow o) = 3 \frac{d\sigma_{ab}}{d\Omega}(o \rightarrow p), \quad (23)$$

$$\frac{d\sigma_{ab}}{d\Omega}(p \rightarrow o + p) = \frac{d\sigma_{ab}}{d\Omega}(o \rightarrow o + p), \quad (24)$$

$$\frac{d\sigma_{ab}}{d\Omega}(p \rightarrow p) = \frac{d\sigma_{ab}}{d\Omega}(p \rightarrow o + p) - \frac{d\sigma_{ab}}{d\Omega}(p \rightarrow o). \quad (25)$$

In this case the Ps beam cannot be polarized, since it is a spin singlet, and the results are independent of the polarization of the H target.

We denote the integrated cross sections corresponding to Eqs. (20)–(25) as  $\sigma_{ab}(o \rightarrow o + p)$ , etc. The total cross section, i.e., the cross section for all possible outcomes, is given by

$$\sigma_{\text{tot}} = \sum_{a,b} \sigma_{ab}(o \rightarrow o + p) = \sum_{a,b} \sigma_{ab}(p \rightarrow o + p) \quad (26)$$

and is the same whether the projectile be *o*-Ps or *p*-Ps.

The primary approximation reported in this paper employs nine H states and nine equivalent Ps states in the expansion (2), we label it 9Ps9H. The nine H states,  $\psi_b(\mathbf{r})$ , are  $1s$ ,  $2s$ , and  $2p$  eigenstates and the  $3s$ ,  $4s$ ,  $3p$ ,  $4p$ ,  $3d$ , and  $4d$  pseudostates of Fon *et al.* [78], they satisfy Eq. (4). The main function of the pseudostates is to represent ionization channels. By rescaling and renormalization according to [79]

$$\phi_a(\mathbf{t}) = \frac{1}{\sqrt{8}} \psi_a(\mathbf{t}/2) \quad (27)$$

TABLE II. PsH binding energies in the different approximations.

Approximation	Energy (eV)
9Ps1H	0.543
22Ps1H	0.634
9Ps9H	0.963
14Ps14H	0.994
Exact [35]	1.067

we generate an equivalent set of eigenstates and pseudostates of Ps satisfying Eq. (3). This set of Ps states has previously been used in frozen target calculations of Ps-H scattering by Campbell *et al.* [27], consistent with the notation used above we label this frozen target approximation 9Ps1H. It is interesting to note that in the 9Ps9H approximation the maximum number of channels for Ps( $1s$ )-H( $1s$ ) scattering is 305, while in the 9Ps1H approximation it is only 16—the practical reason for adopting the frozen target approximation is obvious.

In addition to the 9Ps9H approximation, and for *S*-wave scattering only, we have used an even larger approximation, 14Ps14H. The 14H states correspond to the  $1s$ ,  $2s$ ,  $3s$ , to  $6s$ ,  $2p$ ,  $3p$  to  $6p$  and  $3d$  to  $5d$  states of van Wyngaarden and Walters [80], the 14 Ps states are their counterparts from Eq. (27). These 14 Ps states are a subset of the 22 states used in the frozen target calculations of Campbell *et al.* [27], we label that approximation 22Ps1H.

It should be noted that the 9Ps9H and 14Ps14H approximations both incorporate the van der Waals coefficient,  $C_6 = 34.8$  a.u. [73] [see Eq. (1)], essentially exactly.

The coupled Eqs. (9) have been solved by conversion to partial-wave form, followed by application of the *R*-matrix technique [81].

### III. RESULTS

The lowest *R*-matrix eigenvalue for *S*-wave scattering in the electronic spin singlet state gives the PsH binding energy in the approximation. The calculated energies are shown in Table II. Clearly, there is a major improvement in the binding energy on including excited states of the target atom, but convergence to the last 10% of the exact energy seems to be slow, compare 9Ps9H and 14Ps14H with the exact result.

Next, we consider scattering at very low energies. In this regime effective range theory (ERT) should be applicable. For *S*-wave scattering the ERT expansion takes the form [28]

$$p_0 \cot(\delta_0) = -\frac{1}{a} + \frac{1}{2} r p_0^2 + \dots, \quad (28)$$

where  $\delta_0$  is the *S*-wave phase shift,  $a$  is the scattering length, and  $r$  the effective range. Our results for  $a$  and  $r$  are given in Table III for both singlet and triplet scattering. The present calculations, 9Ps9H and 14Ps14H, are in very good agreement with each other and very close to the scattering lengths obtained by Ivanov, Mitroy, and Varga [31], but about 15% smaller than the scattering lengths of the 22Ps1H frozen tar-



TABLE III. *S*-wave scattering lengths ( $a$ ) and effective ranges ( $r$ ) in units of  $a_0$ . Electronic spin singlet (triplet) quantities are denoted by a + (−) subscript.

	22Ps1H	9Ps9H	14Ps14H	Ref. [31]	Other
$a_+$	5.20	4.48	4.41	4.3	4.5, <sup>a</sup> 5.84, <sup>b</sup> 3.49 <sup>c</sup>
$r_+$	2.52	2.22 <sup>d</sup>	2.19 <sup>d</sup> (2.13) <sup>e</sup>	(2.08) <sup>e</sup>	2.2, <sup>a</sup> 2.90 <sup>b</sup>
$a_-$	2.45	2.06	2.06	2.2	2.36, <sup>a</sup> 2.32, <sup>b</sup> 2.46 <sup>c</sup>
$r_-$	1.32	1.47 <sup>d</sup>	1.47 <sup>d</sup>		1.31 <sup>a</sup>

<sup>a</sup>Stabilization calculation of Drachman and Houston [28,29].

<sup>b</sup>Kohn variational calculation of Page [32].

<sup>c</sup>“Variational” calculation of Adhikari and Mandal [33].

<sup>d</sup>Estimated accuracy 10%.

<sup>e</sup>Calculated from formula (30) as described in the text.

get approximation. Page [32], who gets somewhat larger scattering lengths using the Kohn variational principle, points out that the Kohn principle gives an upper bound on the scattering length. While, strictly speaking, the *R*-matrix method that we use here does not guarantee an upper bound, if only because of the Buttle correction approximation [81], in actual practice it probably does. We have seen in Table II that the 14Ps14H approximation gives a PsH binding energy that is 7% too small. The significance of this bound state to *S*-wave singlet scattering is that it corresponds to a pole in the scattering matrix at an impact energy equal to minus the binding energy. The closer this pole to zero energy, i.e., the smaller the binding energy, the larger the zero energy cross section, i.e.,  $4\pi a_+^2$ , is likely to be, see Fig. 2. We therefore expect that our 14Ps14H value for  $a_+$ , i.e.,  $4.41 a_0$ , is probably marginally too large and so we would recommend the value  $4.3 a_0$  of Inanov, Mitroy, and Varga [31] as more reasonable. The quite low result  $a_+ = 3.49 \pm 0.20 a_0$  of Adhikari and Mandal [33] is not to be regarded as better since, as stated in the introduction, their variational calculation is compromised by the approximation of a Green’s function. For triplet scattering we recommend our own number  $a_- = 2.06 a_0$ .

The effective range values  $r_{\pm}$  in the 9Ps9H and 14Ps14H approximations shown in Table III have been obtained by fitting formula (28) to the calculated low-energy phase shifts. Various fits have been tried, including higher powers of  $p_0$ , but because we do not know the range of validity of Eq. (28) and because it is difficult to get adequate numerical accuracy at low  $p_0$ , the resultant numbers, we estimate, are only accurate to about 10%. For  $r_+$  we get agreement with the much earlier estimate,  $2.2 a_0$ , of Drachman and Houston [28], a number which is smaller than the 22Ps1H frozen target value of  $2.52 a_0$ . By contrast, our present value for  $r_-$  is 12% larger than that of Drachman and Houston [29], the latter agrees very well with the 22Ps1H result.

It is a well-known fact that at a bound-state pole in the scattering matrix  $\cot \delta = i$  [28]. At the pole  $p_0 = i\sqrt{4E_b}$  where  $E_b$  is the binding energy. Assuming that the two-term formula (28) is adequate for extrapolation to the pole, we find that,

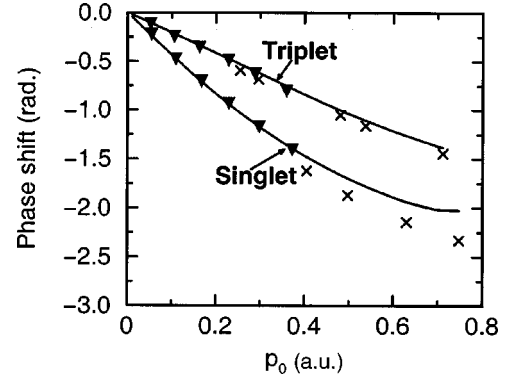


FIG. 1. *S*-wave phase shifts for electronic spin singlet and triplet scattering: curves, 14Ps14H approximation; solid triangles, Ivanov, Mitroy, and Varga [31]; crosses, Drachman and Houston [28,29].

$$E_b = \frac{[(1 - r/a) - \sqrt{1 - 2r/a}]}{2r^2}. \quad (29)$$

Using the values of  $a_+$  and  $r_+$  given in Table III for the 14Ps14H approximation we obtain  $E_b = 1.19$  eV which is 20% higher than the number actually calculated in the approximation, see Table II. From Table III we see that the ratio  $2r_+/a_+$  is close to unity. The problem is that in this situation the formula (29) is very sensitive to the values of  $a_+$  and  $r_+$ . Contrariwise, if we know accurately  $E_b$  and one of either the scattering length or the effective range, then Eq. (29) gives us an accurate way to getting the third value. Now, we have much more confidence in our values for  $a_+$  than for  $r_+$ . Inverting Eq. (29) to read

$$r = \frac{a\sqrt{4E_b} - 1}{2aE_b}, \quad (30)$$

and using  $E_b$  from Table II and  $a_+$  from Table III we calculate, in the 14Ps14H approximation, that a more accurate value for  $r_+$  in this approximation might be  $r_+ = 2.13$  a.u. Using the exact binding energy  $E_b$  from Table II and the preferred scattering length of Ivanov, Mitroy, and Varga from Table III, we obtain  $r_+ = 2.08$  a.u. These numbers differ by no more than 5% from the fitted result  $r_+ = 2.19$  a.u. of the 14Ps14H approximation, which is a comforting level of agreement. It should be noted for triplet scattering that the ratio  $2r_-/a_- > 1$ , Table III, and so no bound state is possible according to Eq. (29), which is indeed the case.

In Fig. 1 we compare our 14Ps14H *S*-wave phase shifts [82] for electronic spin singlet and triplet scattering with the numbers obtained by Ivanov, Mitroy, and Varga [31] and Drachman and Houston [28,29] who have both used the stabilization method. There is good agreement with the phase shifts of Ivanov, Mitroy, and Varga although our singlet (triplet) phase shifts tend to lie marginally lower (higher). The phase shifts of Drachman and Houston sit noticeably below the results of Ivanov, Mitroy, and Varga and the present paper, especially for singlet scattering. While, as noted in connection with Table III, the *R*-matrix method does not guarantee a rigorous bound, in practice it almost certainly gives an accurate lower bound on the phase shift.

TABLE IV.  $S$ -,  $P$ -, and  $D$ -wave phase shifts ( $\delta_0$ ,  $\delta_1$ , and  $\delta_2$ ).  $\delta_0$  has been calculated in the 14Ps14H approximation,  $\delta_1$  and  $\delta_2$  in the 9Ps9H approximation. A superscript + (−) indicates singlet (triplet) scattering. Units are radians. Powers of ten are indicated by superscripts.

$p_0$ (au)	$\delta_0^+$	$\delta_0^-$	$\delta_1^+$	$\delta_1^-$	$\delta_2^+$	$\delta_2^-$
0.05	−0.219	−0.103	$0.264^{-2}$	$−0.763^{-4}$	$0.601^{-5}$	$0.416^{-5}$
0.1	−0.434	−0.206	$0.213^{-1}$	$−0.953^{-3}$	$0.146^{-3}$	$0.848^{-4}$
0.2	−0.834	−0.414	0.175	$−0.122^{-1}$	$0.315^{-2}$	$0.115^{-2}$
0.3	−1.178	−0.624	0.545	$−0.456^{-1}$	$0.165^{-1}$	$0.284^{-2}$
0.4	−1.467	−0.838	0.908	−0.104	$0.495^{-1}$	$0.237^{-2}$
0.5	−1.704	−1.037	1.068	−0.178	0.108	$−0.466^{-2}$
0.6	−1.890	−1.213	1.103	−0.247	0.194	$−0.185^{-1}$
0.7	−2.018	−1.367	1.099	−0.295	0.302	$−0.327^{-1}$

For future reference, we give in Table IV a tabulation of our  $S$ -,  $P$ -, and  $D$ - wave phase shifts in the incident momentum range  $p_0=0.05$  to 0.7 a.u. Noteworthy is the sign change in the triplet  $D$ -wave phase shift,  $\delta_2^-$ , indicating a competition between a net attractive interaction at low  $p_0$ , i.e., large-impact distance, and a net repulsive interaction at smaller impact distances, i.e., higher  $p_0$ .

We turn now to the elastic partial-wave cross sections,  $\sigma_{\text{el}}^{(S_e)}(J)$ , in the electronic spin singlet and triplet states. Our conventions are such that [see Eqs. (13) and (15)]

$$\sum_{J=0}^{\infty} \sigma_{\text{el}}^{(S_e)}(J) = \int |f_{00}^{(S_e)}|^2 d\Omega, \quad (31)$$

where  $J$  labels the total orbital angular momentum. Figs. 2, 3, and 4 show results for the  $S$ ,  $P$ , and  $D$  waves in the 9Ps9H,

9Ps1H, and 22Ps1H approximations. Consider Fig. 2 for  $S$ -wave scattering in the singlet state. Here we see that the zero energy cross section in the 9Ps9H approximation is only 74% of the 22Ps1H frozen target value. This is consistent with the higher PsH binding energy in the 9Ps9H approximation, see Table II, which results in the bound-state pole in the scattering matrix being further away from zero impact energy. At higher energies, Fig. 2(b), we see a single resonance in all three approximations. As described by Drachman [36] this corresponds to an unstable bound state of the positron orbiting the  $\text{H}^-$  ion. In the 9Ps9H approximation this resonance lies at an energy  $E_r$ , of 4.37 eV [83], some 0.18 eV below the resonance in the frozen target 22Ps1H approximation, but still substantially, by 0.36 eV, above the first resonance predicted by Yan and Ho [35]. The width  $\Gamma_r$ , of the resonance in the 9Ps9H approximation is 0.10 eV, the corresponding Yan and Ho prediction being 0.095 eV.

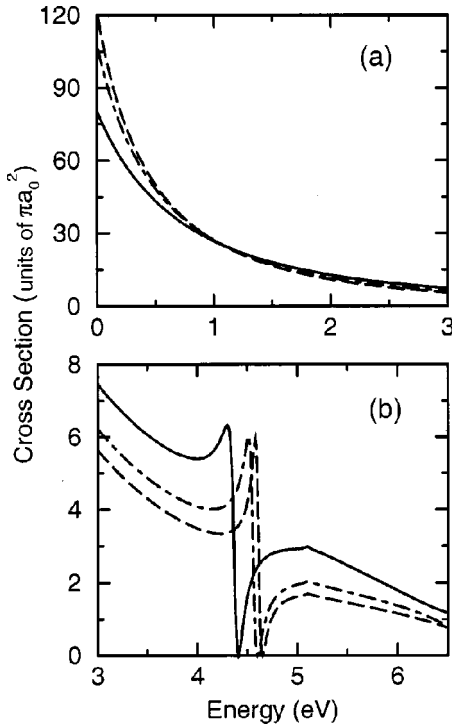


FIG. 2. Electronic spin singlet  $S$ -wave cross section for elastic scattering. Approximations: solid curve, 9Ps9H; dashed curve, 9Ps1H; dash-dot curve, 22Ps1H.

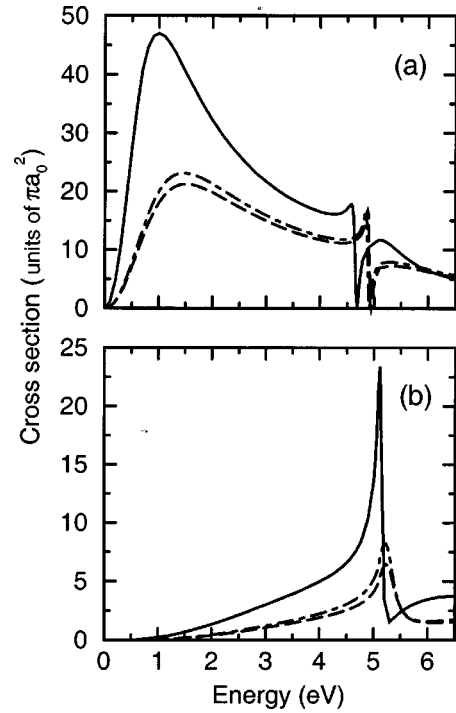


FIG. 3. Electronic spin singlet partial-wave cross sections for elastic scattering: (a)  $P$  wave; (b)  $D$  wave. Approximations: solid curve, 9Ps9H; dashed curve, 9Ps1H; dash-dot curve, 22Ps1H.

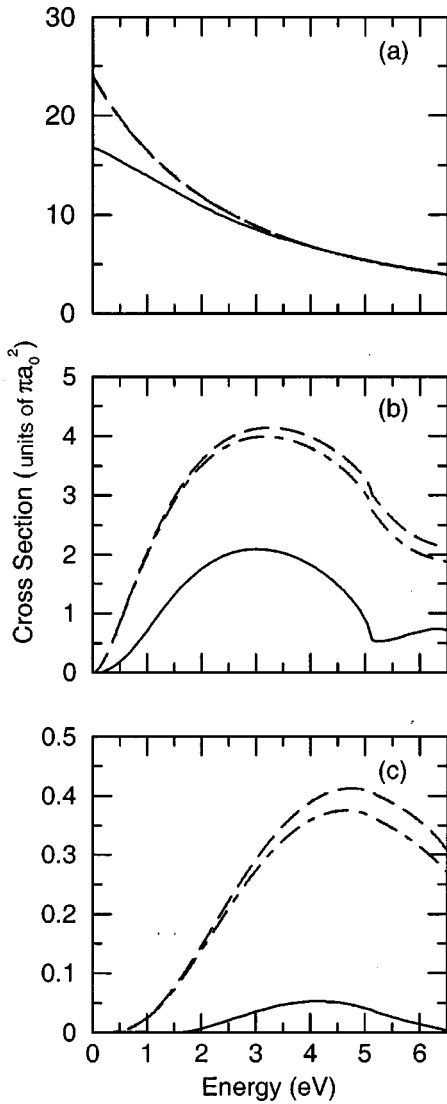


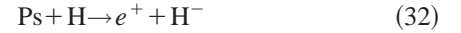
FIG. 4. Electronic spin triplet partial-wave cross sections for elastic scattering: (a)  $S$  wave; (b)  $P$  wave; (c)  $D$  wave. Approximations: solid curve, 9Ps9H; dashed curve, 9Ps1H; dash-dot curve, 22Ps1H.

The changes in the  $P$ -wave singlet cross section on including excited target states are even more spectacular, Fig. 3(a). Here we see that the 9Ps9H cross section rises much more rapidly from threshold than the frozen target cross sections and reaches a peak, near 1 eV, over two times larger. Again, a single resonance is seen at  $E_r=4.66$  eV of width  $\Gamma_r=0.084$  eV. This compares with the frozen target 22Ps1H result  $E_r=4.88$  eV,  $\Gamma_r=0.058$  eV and the first  $P$ -wave resonance of Yan and Ho [37] with  $E_r=4.28$  eV,  $\Gamma_r=0.044$  eV.

In the energy range shown, Fig. 3(b), the  $D$ -wave singlet cross section is very much dominated by the resonance. In the 9Ps9H approximation the resonance is much more pronounced than in the frozen target approximations, its position and width are  $E_r=5.16$  eV,  $\Gamma_r=0.15$  eV. In the 22Ps1H approximation  $E_r=5.28$  eV,  $\Gamma_r=0.47$  eV while the result of Ho and Yan [38] is  $E_r=4.71$  eV,  $\Gamma_r=0.093$  eV.

As pointed out in the Introduction, there should actually

be an infinite series of Rydberg resonances in each singlet partial wave converging on to the threshold for  $H^-$  formation, i.e.,



at 6.05 eV. In a recent paper [40] the present authors have shown this explicitly by adding on to the 22Ps1H frozen target approximation the  $H^-$  formation channel (32). That only one resonance appears in each partial wave in the present paper and in the frozen target approximations indicates that the product expansion (2) is, in practical terms, inadequate for describing the resonant structure. For a proper description of the resonances explicit inclusion of the  $H^-$  formation channel is essential. As shown in [40] the single resonance of the 9Ps9H approximation would appear to give an “average” through the resonance structure.

The significance of the  $H^-$  formation channel goes deeper, however. In connection with Table II we have noted the seemingly slow convergence of the present approach to the PsH binding energy, thus the 14Ps14H approximation is still 7% off the exact value. In [40] it is shown that the mere inclusion of the  $H^-$  channel improves the binding energy in the 22Ps1H approximation by 34% to 0.850 eV. This suggests that the absence of an explicit representation of the  $H^-$  formation channel in Eq. (2) may be at the heart of this slow convergence. Further, it is found that the addition of the  $H^-$  channel to the 22Ps1H frozen target approximation produces a singlet  $P$ -wave cross section very comparable to that of the 9Ps9H approximation shown in Fig. 3(a).

In short, the results of [40] strongly suggest that the main effect of the excited H states in the 9Ps9H approximation for spin singlet scattering is to replicate a virtual  $H^-$  channel, a channel that would be better included explicitly in the approximation. This is an avenue for future work. What is very satisfying is the way [40] seems to corroborate what is presented here. There is another point concerning spin singlet scattering which may be of some importance and which has not so far been investigated, to the best of our knowledge. Besides  $H^-$  formation, we also have the possibility of  $\text{Ps}^-$  formation in singlet scattering. The threshold for this process is 13.3 eV. While virtual  $\text{Ps}^-$  formation may not be as important as  $H^-$  formation, it may still be significant and infinite series of Rydberg resonances converging on to the  $\text{Ps}^-$  formation threshold might, *a priori*, be reasonably expected. This is a matter worthy of investigation.

Let us now look at the spin triplet partial-wave cross sections, these are shown in Fig. 4. Here we see a marked difference between the 9Ps9H numbers and those of the frozen target approximations. There is no obvious physics, such as virtual  $H^-$  or  $\text{Ps}^-$  formation, to which these differences could be attributed. We have remarked in connection with the phase shift  $\delta_2^-$  of Table IV on a competition or cancellation between attractive and repulsive interactions. This competition would seem to be at the heart of the reduced 9Ps9H cross sections seen in Fig. 4. In the triplet state we expect a repulsive contribution from electron exchange as it tries to prevent two electrons with the same spin occupying the same

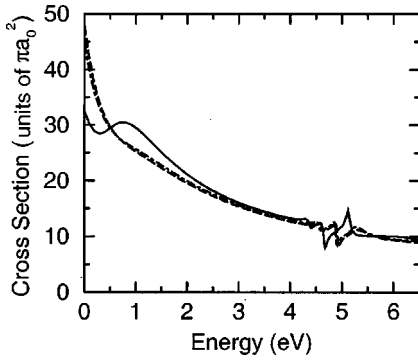


FIG. 5. Total cross section  $\sigma_{\text{tot}}$  see Eq. (26). Approximations: solid curve, 9Ps9H; dashed curve, 9Ps1H; dash-dot curve, 22Ps1H.

space. For an attractive interaction the van der Waals potential (1) is an obvious candidate. This potential can be “switched off” by setting

$$U_{1s1s,npmp}(\mathbf{R}_1) = U_{nmp,1s1s}(\mathbf{R}_1) = 0$$

in Eq. (9) for all  $p$ -states  $np$  and  $mp$  of the Ps and H atom, respectively. This was found to have an insubstantial effect on the 9Ps9H cross sections of Fig. 4. Obviously the situation is more complex. Finally, as expected, we see no resonances in the triplet cross sections in Fig. 4.

In Fig. 5, we show the total cross section  $\sigma_{\text{tot}}$  of Eq. (26). Below 5.1 eV this is just the elastic cross section  $\sigma_{1s1s}(o \rightarrow o+p)$ . At zero energy this cross section is 30% smaller in the 9Ps9H approximation than in the frozen target approximations. Whereas the frozen target cross sections fall rapidly and monotonically with increasing impact energy, the 9Ps9H cross section exhibits a dip at 0.3 eV and a maximum at 0.8 eV. This maximum is clearly a result of the rapid rise and large peak in the  $P$ -wave singlet cross section of Fig. 3(a). Above 2 eV there is a fair degree of similarity between the frozen target and 9Ps9H cross sections except that the resonance structure is a little more pronounced in the 9Ps9H approximation, primarily as a result of the larger  $D$ -wave resonance in the singlet cross section of Fig. 3(b).

Figure 6 shows the  $o$ -Ps( $1s$ )  $\rightarrow$   $p$ -Ps( $1s$ ) conversion cross section  $\sigma_{1s1s}(o \rightarrow p)$ , see Eq. (20). The 9Ps9H cross section is distinguished from the frozen target results by a

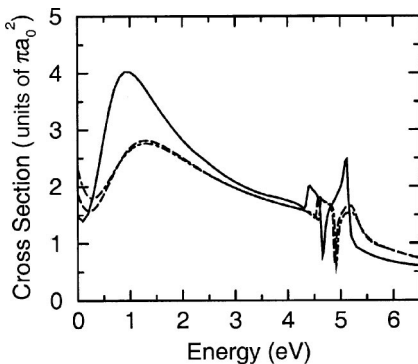


FIG. 6. Cross section for  $o$ -Ps( $1s$ ) to  $p$ -Ps( $1s$ ) conversion. Approximations: solid curve, 9Ps9H; dashed curve, 9Ps1H, dash-dot curve, 22Ps1H.

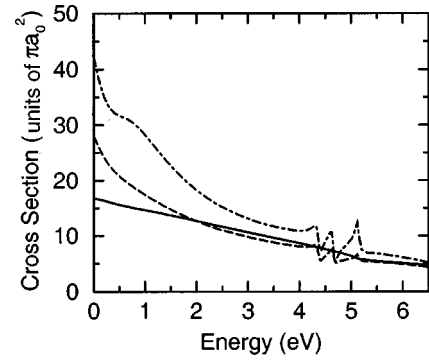


FIG. 7. Integrated cross sections corresponding to  $A$ ,  $C$ , and  $D$  of Eqs. (16), (18), and (19) for elastic scattering: dashed curve,  $A$ ; solid curve,  $C$ ; dash-dot curve,  $D$ .

much larger peak, coming from the singlet  $P$  wave of Fig. 3(a), and larger resonance structure coming from the singlet  $D$  wave of Fig. 3(b).

To complete the picture we show in Fig. 7 the integrated 9Ps9H cross sections corresponding to  $A$ ,  $C$ , and  $D$  of Eqs. (16), (18), and (19) for elastic scattering. These together with Fig. 6 [corresponding to Eq. (17)] specify all possible elastic transitions between spin substates of the Ps and the atom, see Table I.

#### IV. CONCLUSIONS

We have computed cross sections for Ps( $1s$ )-H( $1s$ ) scattering in the impact energy range from 0 to 6.5 eV using a coupled-state approximation which includes excited states of both the Ps and the H atom. This is, by far, the largest calculation so far undertaken within this formalism. With the exception of  $S$ -wave scattering, where an approximation employing 14 states on each center (14Ps14H) has also been used, the calculations have been carried out using nine Ps states and nine H states (9Ps9H). These nine states may be described as  $1s$ ,  $2s$ ,  $\bar{3s}$ ,  $4s$ ,  $2p$ ,  $3p$ ,  $4p$ ,  $3d$ , and  $4d$ , where a “bar” indicates a pseudostate, the primary purpose of the pseudostates being to represent ionization channels.

Good agreement has been obtained with  $S$ -wave scattering lengths and phase shifts recently calculated by Ivanov, Mitroy, and Varga [31] using the stabilization method, while substantial differences are seen from earlier frozen target results. It is clear that inclusion of excited target states is absolutely necessary.

For electronic spin singlet scattering it is found that convergence to the exact PsH bound-state energy is slow, that resonance positions are too high compared with the accurate calculations of Yan and Ho [35,37–39], and that only one resonance, rather than an infinite Rydberg series, appears in each partial wave. It is shown elsewhere [40] that these defects are due to lack of an explicit representation of the  $H^-$  formation channel. Whereas  $H^-$  formation is implicitly included in the expansion (2) when a complete set of states is used, in practice only a finite number of states can be deployed and the product expansion format is then inadequate to the task. Much of the effect of excited target states in singlet scattering at low energies seems to be directed to-



wards virtual  $H^-$  formation. Another formation channel in singlet scattering is  $Ps^-$ , this opens up at 13.3 eV, some 7.3 eV above  $H^-$  formation. While we would expect  $Ps^-$  formation, whether real or virtual, to be less important than  $H^-$  formation, it may yet exert a significant enough effect on low-energy Ps-H scattering and, presumably, also has its own series of Rydberg resonances converging on to 13.3 eV. Investigation of this channel is recommended.

For electronic spin triplet scattering there are also large differences on frozen target calculations but here it is difficult to pin the differences on to an identifiable physical effect such as  $H^-$  or  $Ps^-$  formation which are only possible in singlet scattering. For triplet scattering there seems to be a cancellation going on between attractive and repulsive parts of the interaction. The repulsive part, presumably, derives mainly from the electronic antisymmetry which prevents two electrons with the same spin from occupying the same point in space. The attractive part does not appear to come significantly from the van der Waals force which, *a priori*, would be the obvious candidate. The physics is unclear.

While the work reported in [40] nicely corroborates what

has been presented here, neither is complete in itself. Thus [40] deals only with singlet scattering and is then only a frozen target approximation,  $22Ps1H$ , with the  $H^-$  channel added. It cannot, therefore, represent target excitation effects outside real or virtual  $H^-$  formation and it tells us nothing about triplet scattering. On the other hand, the present calculations deal clumsily with virtual  $H^-$  formation and fail to produce the correct Rydberg resonance structure converging on to the  $H^-$  formation threshold at 6.05 eV, although they do give an average through this structure [40]. It is now clear that a definitive assault on Ps-H scattering should include excited states of both the target and the Ps as well as explicit representation of the  $H^-$  formation channel and possibly also of the  $Ps^-$  channel. That is a task for the future.

#### ACKNOWLEDGMENTS

This work was supported by EPSRC Grant Nos. GR/NO7424 and GR/MO1784. We are also indebted to Dr. G. Laricchia for informative discussions on Ps beams.

- 
- [1] G. Laricchia, M. Charlton, T. C. Griffith, and F. M. Jacobsen, in *Positron (Electron)-Gas Scattering*, edited by W. E. Kaupila, T. S. Stein, and J. M. Wadehra (World Scientific, Singapore, 1986), p. 313.
- [2] G. Laricchia, M. Charlton, S. A. Davies, C. D. Beling, and T. C. Griffith, *J. Phys. B* **20**, L99 (1987).
- [3] M. Charlton and G. Laricchia, *J. Phys. B* **23**, 1045 (1990).
- [4] M. Charlton and G. Laricchia, *Comments At. Mol. Phys.* **26**, 253 (1991).
- [5] N. Zafar, G. Laricchia, M. Charlton, and T. C. Griffith, *J. Phys. B* **24**, 4661 (1991).
- [6] G. Laricchia, N. Zafar, M. Charlton, and T. C. Griffith, *Hyperfine Interact.* **73**, 133 (1992).
- [7] N. Zafar, G. Laricchia, and M. Charlton, *Hyperfine Interact.* **89**, 243 (1994).
- [8] G. Laricchia, *Nucl. Instrum. Methods Phys. Res. B* **99**, 363 (1995).
- [9] N. Zafar, G. Laricchia, M. Charlton, and A. Garner, *Phys. Rev. Lett.* **76**, 1595 (1996).
- [10] A. J. Garner, G. Laricchia, and A. Özen, *J. Phys. B* **29**, 5961 (1996).
- [11] G. Laricchia, *Hyperfine Interact.* **100**, 71 (1996).
- [12] A. J. Garner and G. Laricchia, *Can. J. Phys.* **74**, 518 (1996).
- [13] A. J. Garner, A. Özen, and G. Laricchia, *Nucl. Instrum. Methods Phys. Res. B* **143**, 155 (1998).
- [14] A. J. Garner, A. Özen, and G. Laricchia, *J. Phys. B* **33**, 1149 (2000).
- [15] A. Özen, A. J. Garner, and G. Laricchia, *Nucl. Instrum. Methods Phys. Res. B* **171**, 172 (2000).
- [16] H. R. J. Walters, J. E. Blackwood, and M. T. McAlinden, in *New Directions in Antimatter Chemistry and Physics*, edited by C. M. Surko and F. A. Gianturco (Kluwer, Dordrecht, 2001), p. 173.
- [17] K. F. Canter, J. D. McNutt, and L. O. Roellig, *Phys. Rev. A* **12**, 375 (1975).
- [18] P. G. Coleman, S. Rayner, F. M. Jacobsen, M. Charlton, and R. M. West, *J. Phys. B* **27**, 981 (1994).
- [19] Y. Nagashima, M. Kakimoto, T. Hyodo, K. Fujiwara, A. Ichimura, T. Chang, J. Deng, T. Akahani, T. Chiba, K. Suzuki, B. T. A. McKee, and A. T. Stewart, *Phys. Rev. A* **52**, 258 (1995).
- [20] Y. Nagashima, T. Hyodo, K. Fujiwara, and I. Ichimura, *J. Phys. B* **31**, 329 (1998).
- [21] M. Skalsey, J. J. Engbrecht, R. K. Bithell, R. S. Vallery, and D. W. Gidley, *Phys. Rev. Lett.* **80**, 3727 (1998).
- [22] Unless otherwise stated, it is assumed that we are talking about collisions in which ground-state Ps is incident upon ground-state H, i.e.,  $Ps(1s)-H(1s)$  collisions.
- [23] H. S. W. Massey and C. B. O. Mohr, *Proc. Phys. Soc., London, Sect. A* **67**, 695 (1954).
- [24] M. T. McAlinden, F. G. R. S. MacDonald, and H. R. J. Walters, *Can. J. Phys.* **74**, 434 (1996).
- [25] P. A. Fraser, *Proc. Phys. Soc. London* **78**, 329 (1961); S. Hara and P. A. Fraser, *J. Phys. B* **8**, L472 (1975).
- [26] H. Ray and A. S. Ghosh, *J. Phys. B* **29**, 5505 (1996); **30**, 3745 (1997).
- [27] C. P. Campbell, M. T. McAlinden, F. G. R. S. MacDonald, and H. R. J. Walters, *Phys. Rev. Lett.* **80**, 5097 (1998).
- [28] R. J. Drachman and S. K. Houston, *Phys. Rev. A* **12**, 885 (1975).
- [29] R. J. Drachman and S. K. Houston, *Phys. Rev. A* **14**, 894 (1976).
- [30] F. E. Harris, *Phys. Rev. Lett.* **19**, 173 (1967); H. H. Michels and F. E. Harris, *ibid.* **19**, 885 (1967); A. U. Hazi and H. S. Taylor, *Phys. Rev. A* **1**, 1109 (1970).
- [31] I. A. Ivanov, J. Mitroy, and K. Varga, *Phys. Rev. Lett.* **87**, 063201 (2001).
- [32] B. A. P. Page, *J. Phys. B* **9**, 1111 (1976).
- [33] S. K. Adhikari and P. Mandal, *J. Phys. B* **34**, L187 (2001).

- [34] A. Ore, Phys. Rev. **83**, 665 (1951).
- [35] Z-C. Yan and Y. K. Ho, Phys. Rev. A **59**, 2697 (1999).
- [36] R. J. Drachman, Phys. Rev. A **19**, 1900 (1979).
- [37] Z-C. Yan and Y. K. Ho, Phys. Rev. A **57**, R2270 (1998).
- [38] Y. K. Ho and Z-C. Yan, J. Phys. B **31**, L877 (1998).
- [39] Y. K. Ho and Z-C. Yan, Phys. Rev. A **62**, 052503 (2000).
- [40] J. E. Blackwood, M. T. McAlinden, and H. R. J. Walters, Phys. Rev. A (to be published).
- [41] Y. K. Ho, Phys. Rev. A **41**, 68 (1990).
- [42] S. Sur, S. K. Adhikari, and A. S. Ghosh, Phys. Rev. A **53**, 3340 (1996).
- [43] P. K. Sinha, P. Chaudhury, and A. S. Ghosh, J. Phys. B **30**, 4643 (1997).
- [44] P. K. Sinha and A. S. Ghosh, Phys. Rev. A **58**, 242 (1998).
- [45] P. K. Biswas and S. K. Adhikari, J. Phys. B **31**, 3147 (1998); **31**, 5404 (1998).
- [46] H. Ray and A. S. Ghosh, J. Phys. B **31**, 4427 (1998).
- [47] A. S. Ghosh, P. K. Sinha, and H. Ray, Nucl. Instrum. Methods Phys. Res. B **143**, 162 (1998).
- [48] N. K. Sarkar, P. Chaudhury, and A. S. Ghosh, J. Phys. B **32**, 1657 (1999).
- [49] H. Ray, J. Phys. B **32**, 5681 (1999).
- [50] P. K. Biswas and S. K. Adhikari, Phys. Rev. A **59**, 363 (1999).
- [51] S. K. Adhikari and P. K. Biswas, Phys. Rev. A **59**, 2058 (1999).
- [52] S. K. Adhikari, P. K. Biswas, and R. A. Sultanov, Phys. Rev. A **59**, 4829 (1999).
- [53] J. E. Blackwood, C. P. Campbell, M. T. McAlinden, and H. R. J. Walters, Phys. Rev. A **60**, 4454 (1999).
- [54] J. E. Blackwood, C. P. Campbell, M. T. McAlinden, and H. R. J. Walters, in *The Physics of Electronic and Atomic Collisions*, edited by Y. Itikawa, K. Okuno, H. Tanaka, A. Yagishita, and M. Matsuzawa, AIP Conf. Proc. No. 500 (AIP, New York, 2000), p. 454.
- [55] P. K. Biswas and S. K. Adhikari, J. Phys. B **33**, 1575 (2000).
- [56] P. K. Sinha, A. Basu, and A. S. Ghosh, J. Phys. B **33**, 2579 (2000).
- [57] H. Ray, J. Phys. B **33**, 4285 (2000).
- [58] P. K. Biswas, Phys. Rev. A **61**, 012502 (2000).
- [59] S. K. Adhikari, Phys. Rev. A **62**, 062708 (2000).
- [60] P. K. Biswas and S. K. Adhikari, Chem. Phys. Lett. **317**, 129 (2000).
- [61] P. K. Biswas, Nucl. Instrum. Methods Phys. Res. B **171**, 135 (2000).
- [62] P. K. Biswas, Radiat. Phys. Chem. **58**, 443 (2000).
- [63] S. K. Adhikari and P. Mandal, J. Phys. B **34**, 1361 (2001).
- [64] A. Basu, P. K. Sinha, and A. S. Ghosh, Phys. Rev. A **63**, 012502 (2001).
- [65] A. S. Ghosh, A. Basu, T. Mukherjee, and P. K. Sinha, Phys. Rev. A **63**, 042706 (2001).
- [66] A. Basu, P. K. Sinha, and A. S. Ghosh, Phys. Rev. A **63**, 052503 (2001).
- [67] S. K. Adhikari, Phys. Rev. A **63**, 054502 (2001).
- [68] S. K. Adhikari, Phys. Lett. A **283**, 224 (2001).
- [69] S. K. Adhikari, Nucl. Phys. A **684**, 666C (2001).
- [70] A. S. Ghosh and P. K. Sinha, in *New Directions in Antimatter Chemistry and Physics*, edited by C. M. Surko and F. A. Gianturco (Kluwer, Dordrecht, 2001), p. 323.
- [71] We use the term “excitation” generically to include both discrete excitations and ionization.
- [72] Assuming the appropriate states of the target and the Ps are included in the expansion (2).
- [73] D. W. Martin and P. A. Fraser, J. Phys. B **13**, 3383 (1980).
- [74] P. Van Reeth and J. W. Humberston, J. Phys. B **28**, L23 (1995).
- [75] C. P. Campbell, M. T. McAlinden, A. A. Kernoghan, and H. R. J. Walters, Nucl. Instrum. Methods Phys. Res. B **143**, 41 (1998).
- [76] Unit vectors are denoted by a “hat.”
- [77] Simply use Table I taking the fractions of the *o*-Ps beam in the states  $m_{Ps} = +1, 0,$  and  $-1$  to be  $a, b,$  and  $c,$  respectively, where  $a + b + c = 1$ .
- [78] W. C. Fon, K. A. Berrington, P. G. Burke, and A. E. Kingston, J. Phys. B **14**, 1041 (1981).
- [79] A. A. Kernoghan, M. T. McAlinden, and H. R. J. Walters, J. Phys. B **28**, 1079 (1995).
- [80] W. L. van Wyngaarden and H. R. J. Walters, J. Phys. B **19**, 929 (1986).
- [81] P. G. Burke and W. D. Robb, Adv. At. Mol. Phys. **11**, 143 (1975).
- [82] These differ little from the 9Ps9H values but are marginally better.
- [83] In the 14Ps14H approximation we obtain a position and width for this resonance of 4.31 and 0.11 eV, respectively.